Ralph Levy (SM'64–F'73) was born in London, England, on April 12, 1932. He received the M.A. degree in physics from St. Catharine's College, Cambridge University, Cambridge, England, in 1953, and the Ph.D. degree in electrical engineering from the University of London, London, England, in 1966.

From 1953 to 1959, he was a Member of the Scientific Staff at the Applied Electronics Laboratories of the General Electric Company, Stanmore, Middlesex, England, where he worked on guided missile, radar, and countermeasures systems, and on microwave components. In 1959, he joined Mullard Research Laboratories, Redhill, Surrey, England, and developed some now widely used techniques in ECM, such as instantaneous frequency measurement (digital IFM), and very broad-band directional couplers. From 1964 to 1967 he was a member of the faculty at Leeds University, and carried out research in microwave network synthesis, including realizations of distributed elliptic function filters, and exact synthesis techniques for branch guide and multi-aperture directional couplers. Since 1967, he has been with Microwave Development Laboratories, Natick, MA., as Research Vice President. He has developed practical techniques for designing very broad band mixed lumped and distributed circuits, and synthesis and field theory techniques to facilitate the design of a variety of microwave components.

Dr. Levy is a member of the Institution of Electrical Engineers (London).

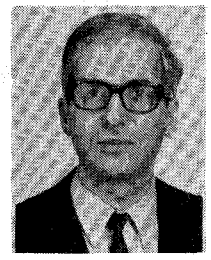

Joseph Helszajn (M'64) was born in Brussels, Belgium, in 1934. He received the Full Technological Certificate of the City and Guilds of London Institute from Northern Polytechnic, London, England in 1955, the M.S.E.E. degree from the University of Santa Clara, Santa Clara, CA, in 1964, the Ph.D. degree from the University of Leeds, Leeds, England, in 1969, and the D.Sc. degree from Heriot-Watt University, Edinburgh, Scotland, in 1976.

He has held a number of positions in the microwave industry. From 1964 to 1966, he was Product Line Manager at Microwave Associates, Inc., Burlington, MA. He is currently a Reader at Heriot-Watt University. He is the author of the books *Principles of Microwave Ferrite Engineering* (New York: Wiley, 1969), *Nonreciprocal Microwave Junctions and Circulators* (New York: Wiley, 1975), and *Passive and Active Microwave Circuits* (New York: Wiley, 1978).

Dr. Helszajn is a fellow of the Institution of Electronic and Radio Engineers (England). In 1968, he was awarded the Insignia Award of the City and Guilds of London Institute.

Noise in Broad-Band GaAs MESFET Amplifiers with Parallel Feedback

KARL B. NICLAS, SENIOR MEMBER, IEEE

Abstract—**The influence of the circuit elements of a single-ended feedback amplifier module on noise figure and gain, as well as on input and output reflection coefficients is discussed. Theoretical results are supported by tests performed on a five-stage single-ended amplifier. The unit exhibits 41.5±0.8 dB of small-signal gain and a maximum noise figure of 4.0 dB between 2.4 and 8.0 GHz. Maximum reflection coefficients of 1.7:1 for the input and 1.5:1 for the output terminal were measured. The unit's overall circuit dimensions are 25×3.6 mm.**

I. Introduction

RECENT ADVANCES in the performance of single-ended microwave feedback amplifiers have resulted in a device that promises to challenge the conventional type amplifier in many applications. This is especially the case whenever compact size and low cost are a factor in broad-band microwave amplification [1], [2]. In addition to multi-octave bandwidths and low-reflection coefficients, the feedback amplifier shows great potential for low-noise applications. This is true in spite of the thermal noise injected by the feedback resistor.

The influence of reactive feedback on the noise figure of microwave amplifiers has been studied by several researchers [3]–[5]. It has also been pointed out that reactive feedback reduces the minimum noise figure of microwave amplifiers, a fact that has been known to designers of VHF amplifiers for several decades [6].

This paper addresses the noise in broad-band microwave amplifiers with parallel feedback. Formulas for the equivalent noise parameters and noise figure of such amplifiers are presented. They take into account the thermal noise agitation of the resistor in the feedback loop. Based on these theoretical solutions, the influence of the circuit elements on noise figure, gain, and reflection coefficients of a practical amplifier are discussed. Attention is focused on

Manuscript received June 24, 1981; revised August 11, 1981.
The author is with Watkins-Johnson Company, Palo Alto, CA 94304.

0018-9480/82/0100-0063$00.75 ©1982 IEEE

the function of the *drain transmission line*, i.e., the line element between the transistor's output port and the node where the feedback loop is connected and its importance for the amplifier's overall performance is studied. The paper attempts to provide the designer of low-noise feedback amplifiers with the information necessary to make a decision on the compromise that exists between gain, gain flatness, noise figure, and reflection loss.

Finally, experimental results measured on a five-stage amplifier are discussed that clearly show the influence of the feedback, resistor on overall and minimum noise figure. The single-ended unit exhibits a minimum gain of 40.7 dB and a maximum noise figure of 4.0 dB between 2.4 and 8.0 GHz.

II. Noise Parameters and Noise Figure

A. Transformation Formulas

Over the last decade a number of papers on the subject of equivalent noise parameters and noise figure in or applicable to feedback amplifiers have been published [3], [4], [7], [8]. While [3] and [4] describe computer results for amplifiers employing reactive feedback,[7] and [8] present formulas for the equivalent noise parameters of general two-ports. The formulas given in this chapter and those developed in the Appendix were derived by essentially following the procedures outlined in [9] and [10]. They take into account the thermal noise agitation injected by the resistor of the feedback loop.

The circuit diagram of the basic feedback amplifier is shown in Fig. 1(a). In order to analyze the noise behavior of the amplifier, the diagram of Fig. 1(a) is converted into the equivalent circuit of Fig. 1(b). The latter contains the voltage noise source v_T and the current noise source i_T of the MESFET, as well as the thermal noise voltage v_{FB} of the feedback resistor. v_{FB} is not correlated to the transistor's noise sources. The MESFET itself is represented by a T-shaped network with one voltage source.

For reasons of simplification, it is beneficial to divide the problem into two parts, i.e., first develop the formulas for the open-loop amplifier and then add the feedback admittance with its thermal noise source. Since all transformation elements of the open-loop case are assumed noiseless, the first part is relatively straightforward when following the steps outlined in the literature [9], [10].

Eliminating the feedback reduces the equivalent circuit of Fig. 1(b) to that of Fig. 2(a). Its equivalent noise resistor R_n, equivalent noise conductance G_n, and correlation admittance Y_{cor}, are

$$R_n = \frac{\overline{|v_1|^2}}{4kT_0\Delta f} = R_n^T|1+jX_GY_{cor}^T|^2 + G_n^TX_G^2 \tag{1a}$$

$$G_n = \frac{\overline{|i_n|^2}}{4kT_0\Delta f} = \frac{G_n^TR_n^T}{R_n^T|1+X_GY_{cor}^T|^2 + G_n^TX_G^2} \tag{1b}$$

$$Y_{cor} = \frac{\overline{i_1v_1^*}}{\overline{|v_1|^2}} = \frac{R_n^T(Y_{cor}^T - jX_G|Y_{cor}^T|^2) - jX_GG_n^T}{R_n^T|1+X_GY_{cor}^T|^2 + G_n^TX_G^2} \tag{1c}$$

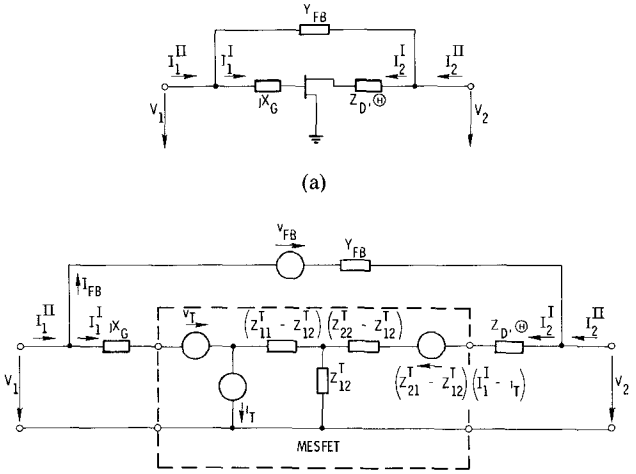

Fig. 1. The basic feedback amplifier. (a) Circuit diagram. (b) Equivalent circuit with noise voltage and noise current sources.

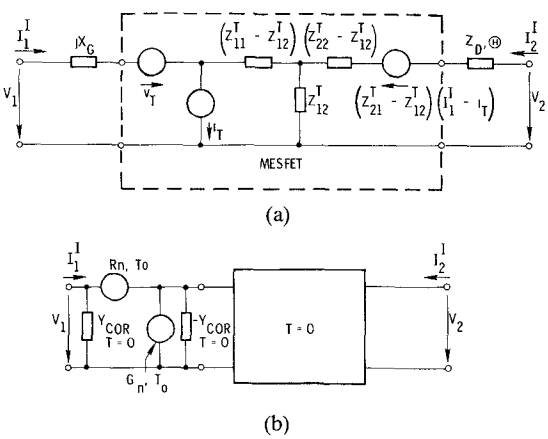

Fig 2. Equivalent circuit of the amplifier with open feedback loop. (a) Two-port representation including the transistor's external noise sources v_T and i_T. (b) Two-port with correlation admittance Y_{cor} and uncorrelated noise sources R_n and G_n.

where

k Boltzmann's constant,
Δf bandwidth,
T_0 absolute temperature in K.
(Superscript T indicates MESFET parameters.)

The equivalent noise parameters are located externally to the noiseless two-port, as shown in Fig. 2(b).

The noise figure of a device is given by

$$F = 1 + \frac{1}{G_s}\left(G_n + R_n|Y_s + Y_{cor}|^2\right). \tag{2a}$$

The minimum noise figure

$$F_{min} = 1 + 2R_n(G_{cor} + G_{s\,min}) \tag{2b}$$

occurs at

$$G_{s\,min} = \sqrt{\frac{G_n}{R_n} + G_{cor}^2} \qquad B_{s\,min} = -B_{cor} \tag{2c}$$

$Y_s = G_s + jB_s$ — signal source admittance.

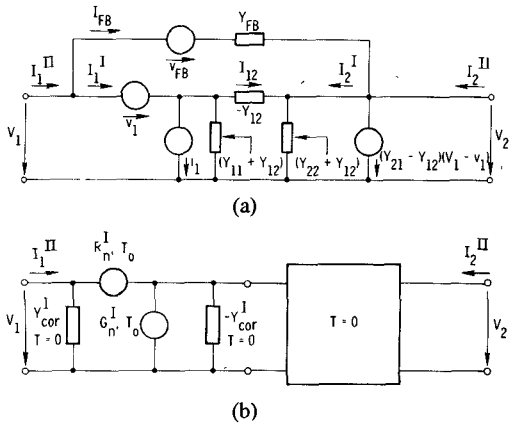

Fig. 3. Equivalent circuit of the feedback amplifier. (a) Two-port representation including the external noise sources v_1 and i_1 of the open-loop amplifier. (b) Two-port with correlation admittance Y_{cor}^I and uncorrelated noise sources R_n^I and G_n^I.

Substituting (1) into (2b) and (2c) demonstrates the well-known fact that the minimum noise figure of a device remains unchanged when it is preceded by a lossless passive two-port.

We now add the parallel feedback in accordance with Fig. 1(b). It consists of the feedback admittance Y_{FB} and the thermal noise source of the feedback resistor v_{FB}. For reasons of simplification, the impedance representation of the open-loop case is converted into its admittance representation resulting in the circuit diagram of Fig. 3(a).

The following relationship exists between the equivalent noise voltages and currents of Fig. 3(a) and the MESFET's noise parameters:

$$v_1 = v_T + jX_G i_T \tag{3a}$$

$$i_1 = i_T = i_n^T + Y_{cor}^T v_T \tag{3b}$$

$$\overline{|v_1|^2} = |1 + jX_G Y_{cor}^T|^2 \overline{|v_T|^2} + X_G^2 \overline{|i_n^T|^2} \tag{3c}$$

$$\overline{|i_1|^2} = \overline{|i_n^T|^2} + |Y_{cor}^T|^2 \overline{|v_T|^2} \tag{3d}$$

where i_n^T is the noncorrelated portion of the MESFET's equivalent noise current.

The transformation formulas for the equivalent noise parameters of the basic feedback amplifier of Fig. 1 have been developed in the Appendix and are based on the circuit diagram of Fig. 3(a). The resulting noise parameters are located externally to the noiseless two-port in accordance with Fig. 3(b). They are

$$R_n^I = \frac{\overline{|v_1^I|^2}}{4kT_0\Delta f} = \left|\frac{Y_{21}}{Y_{21}-Y_{FB}}\right|^2 \left(R_n + \left|\frac{Y_{FB}}{Y_{21}}\right|^2 R_{FB}\right) \tag{4a}$$

$$G_n^I = \frac{\overline{|i_n^I|^2}}{4kT_0\Delta f} = G_n + |Y_{11}+Y_{21}-Y_{cor}|^2 \frac{\left|\frac{Y_{FB}}{Y_{21}}\right|^2 R_n R_{FB}}{R_n + \left|\frac{Y_{FB}}{Y_{21}}\right|^2 R_{FB}} \tag{4b}$$

and

$$Y_{cor}^I = \frac{\overline{i_1^I (v_1^I)^*}}{\overline{|v_1^I|^2}} = Y_{cor} + (Y_{11}+Y_{21}-Y_{cor}) \frac{\frac{Y_{FB}}{Y_{21}} R_n + \left|\frac{Y_{FB}}{Y_{21}}\right|^2 R_{FB}}{R_n + \left|\frac{Y_{FB}}{Y_{21}}\right|^2 R_{FB}} \tag{4c}$$

with

$$Y_{21} = \frac{Z_{21}^T}{(Z_{11}^T Z_{22}^T - Z_{12}^T Z_{21}^T)\cos\Theta + j(Z_{11}^T + jX_G)Z_D \sin\Theta} \tag{5a}$$

$$Y_{11}+Y_{21} = \frac{Z_{21}^T + Z_{22}^T \cos\Theta + jZ_D \sin\Theta}{(Z_{11}^T Z_{22}^T - Z_{12}^T Z_{21}^T)\cos\Theta + j(Z_{11}^T + jX_G)Z_D \sin\Theta}. \tag{5b}$$

It is evident from these formulas that the *drain transmission line* with its characteristic impedance Z_D and electrical length Θ has a significant influence on the minimum noise figure of the amplifier.

In addition, (4b) points out that the presence of a finite feedback resistance always increases the equivalent noise conductance G_n^I. In contrast, R_n^I can theoretically be made smaller than

$$\left(R_n + \left|\frac{Y_{FB}}{Y_{21}}\right|^2 R_{FB}\right)$$

or even R_n through the right choice of Y_{FB}. Since in practical cases, however $Y_{21} \gg Y_{FB}$ a reduction in R_n^I may only be achieved for reactive feedback, i.e., $R_{FB} = 0$.

In this case we find that

$$R_n^I = \left|\frac{Y_{21}}{Y_{21}-Y_{FB}}\right|^2 R_n \tag{6a}$$

$$G_n^I = G_n \tag{6b}$$

$$Y_{cor}^I = Y_{cor}\left(1 - \frac{Y_{FB}}{Y_{21}}\right) + Y_{FB}\left(1 + \frac{Y_{11}}{Y_{21}}\right). \tag{6c}$$

B. Influence of Feedback Admittance and Drain Transmission Line

The influence of the feedback resistor R_{FB} and the electrical length Θ of the high-impedance (90-Ω) drain transmission line on noise figure is of major interest. Both parameters, as will be pointed out in the next chapter, also have significant impact on gain, gain flatness, and VSWR. The circuit elements of the basic feedback amplifier to be analyzed are shown in Fig. 4 which also lists the element values of the transistor model. The latter differ slightly from those of earlier runs [2].

The equivalent noise parameters of the WJ-F810 (R_n^T,

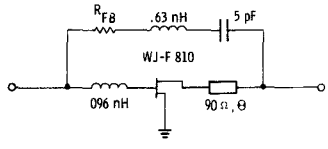

(a)

Equivalent Circuit Elements of WJ-F 810

g_m = 57 mS	R_g = 2.0 ohms
τ_0 = 4 p sec	L_g = 208 nH
C_{gs} = .508 pF	R_s = 1.0 ohms
C_{gd} = .041 pF	L_s = .169 nH
C_{dc} = .035 pF	C_{ds} = .136 pF
R_{gs} = 5.6 ohms	R_d = 2 ohms
R_{ds} = 257 ohms	L_d = 146 nH

(b)

Fig. 4. Circuit elements of the basic amplifier and transistor model. (a) Schematic of amplifier. (b) Equivalent circuit elements of WJ-F810 ($V_{DS}=4$V, $V_{GS}=-0.6$V, $I_{DS}=38.5$ mA).

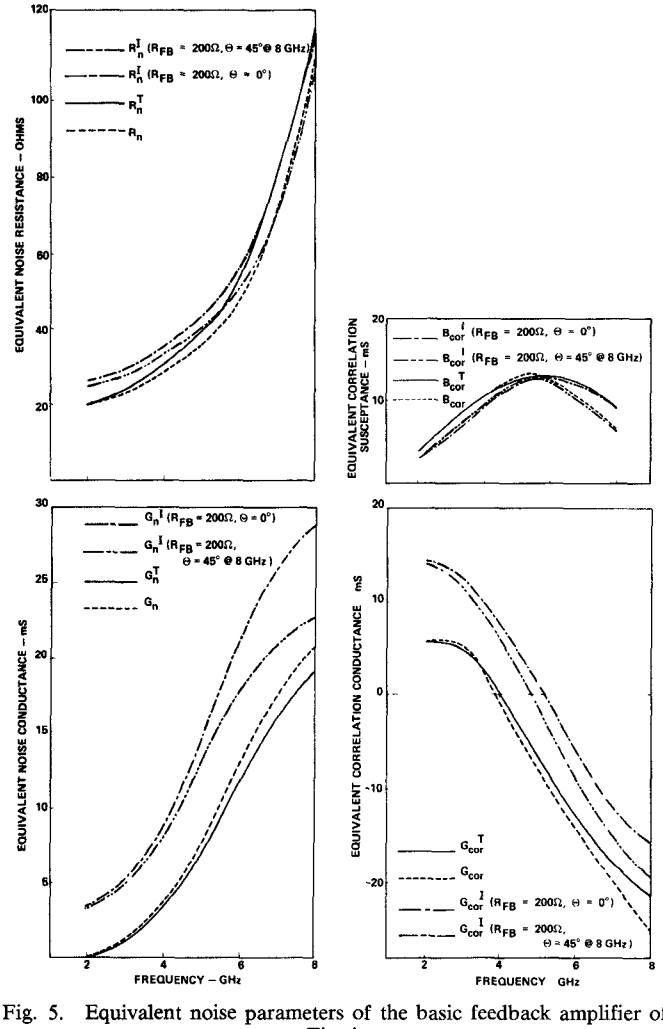

Fig. 5. Equivalent noise parameters of the basic feedback amplifier of Fig. 4.

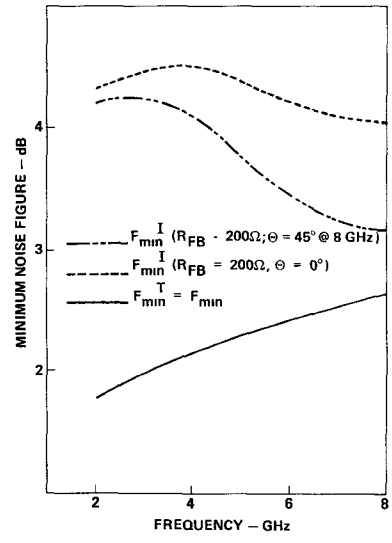

Fig. 6. Minimum noise figure of the basic feedback amplifier of Fig. 4.

G_n^T, G_{cor}^T, and B_{cor}^T) have been calculated using the measured values of the minimum noise figure $F_{\min}$, the noise figure for a 50-Ω source impedance $F(50\ \Omega)$, and the source admittance for minimum noise figure $Y_{s\min}$. They are plotted as solid curves in Fig. 5. The dashed curves demonstrate the influence of the gate lead inductance (0.096 nH) on the noise parameters of the open-loop amplifier across the 2–8-GHz frequency band. While the gate inductance changes the noise parameters and thereby the noise figure F, it does not, as discussed earlier, alter the minimum noise figure $F_{\min}$.

A resistance of $R_{\text{FB}}=200\ \Omega$ was chosen to demonstrate the effect of parallel feedback. This value represents a practical compromise between VSWR, gain, and noise figure performance for our amplifier's input stage. Greater resistance values, as will be described in the following chapter, decrease the noise figure and increase the gain, but also increase the reflection coefficients at the input and output terminals. In order to demonstrate to what degree the electrical length Θ affects the noise figure, two different lengths ($\Theta=0$ and $\Theta=45°$ at 8 GHz) were chosen. While $\Theta=45°$ is not the optimal length for best noise figure, it represents a good compromise between noise figure, VSWR, gain, and stability of the amplifier module. The results are plotted in Fig. 5. The curves clearly display the increases in the equivalent noise resistor R_n^I, noise conductance G_n^I and correlation conductance G_{cor}^I caused by the feedback resistor. This is especially the case at low frequencies where the negative feedback is strongest. In addition, the curves for the case of $\Theta=45°$ exhibit lower noise parameters than those for which $\Theta=0°$, especially towards higher frequencies. The minimum noise figures are compared in Fig. 6. The difference between the open-loop case and that of parallel feedback for $\Theta=0°$ is in excess of 2 dB across the lower octave of the band. It is significantly reduced for $\Theta=45°$ over the second octave of the frequency range.

III. Gain, Reflection Coefficients, and Noise Figure of Practical Amplifiers

A. Characteristics and Performance Tradeoffs

As is the case in most practical amplifier designs, the noise figure of a feedback amplifier cannot be optimized

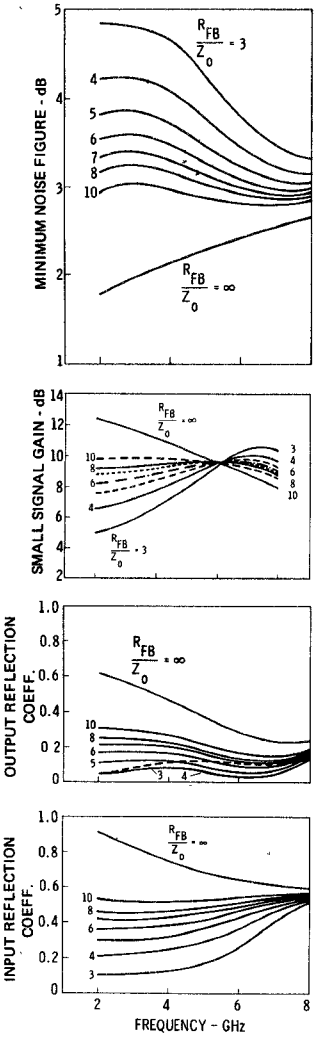

Fig. 7. Minimum noise figure, small-signal gain and VSWR as function of frequency with R_{FB}/Z_0 as parameter ($\Theta = 45°$ at 8 GHz).

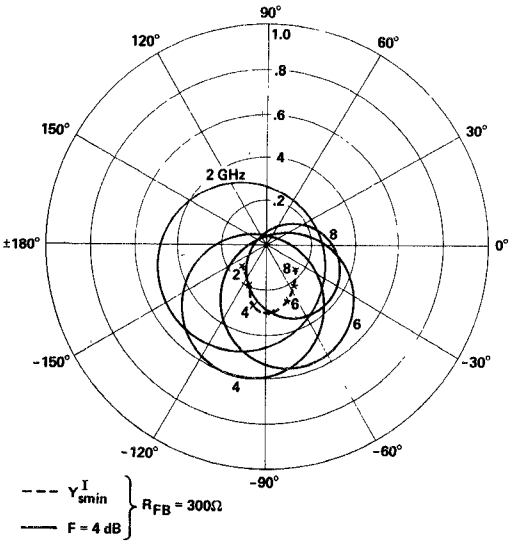

Fig. 8. Optimum matching conditions for noise figure and circles of constant noise ($F = 4$ dB).

without sacrificing other important performance characteristics such as gain, gain flatness, input and output reflection coefficients, as well as stability. This chapter briefly addresses possible options and tradeoffs in the amplifier's performance.

The curves plotted in Fig. 7 represent the minimum noise figure, small-signal gain, and reflection coefficients of the basic feedback amplifier of Fig. 4 for different values of R_{FB}/Z_0. The length of the drain transmission line is 0.185 in or $\Theta = 45°$ at 8 GHz. It is clearly evident from these curves that low-noise figure and high small-signal gain go contrary to low reflection losses. High reflection losses, in turn, severely limit the capability of broad-band multistage amplification.

Another important feature of the feedback amplifier is the proximity of its matching conditions for optimum noise figure and best VSWR. Most important, a compromise between gain and noise figure match results in acceptable broad-band performance of both gain and noise figure. Fig. 8 shows the location of the optimum source admittance Y_{smin} for $R_{FB} = 300\ \Omega$. Also plotted are the circles of constant noise figures $F = 4$ dB. They indicate that between 2 and 8 GHz the maximum noise figure does not exceed $F = 4$ dB for the source admittance $Y_s = Y_0 = Z_0^{-1}$. The minimum gain for the source impedance Z_0 and a load impedance of Z_0 is $G = 8.2$ dB, which is quite acceptable for practical applications.

B. Test Results

The measurements discussed in this section were performed on a five-stage feedback amplifier designed for 2–8-GHz operation. The unit is a member of a family of multistage single-ended amplifiers reported elsewhere [1]. A photograph of the amplifier whose overall circuit dimensions are 25.0×3.6 mm is shown in Fig. 9.

Small-signal gain, noise figure, and VSWR at the input and output terminal are presented in Fig. 10. These performance characteristics demonstrate the potential of the single-ended feedback amplifier as a wide-band and compact low-noise device.

In order to compare theoretical and measured results, an attempt was made to extract the noise figure and the minimum noise figure of the input stage from test data of the five-stage amplifier. The possible error in this process is relatively small due to the high gain of the input stage and the low-noise figure of the subsequent stages. The transformation of the second stage noise parameters performed by the interstage matching network was taken into account. The results which were computed using COMPACT are supplied in Fig. 11. The curves show the noise figure and the minimum noise figure of the input stage and are based on measurements of the identical parameters made on the five-stage unit. The influence of the feedback resistor R_{FB} on the module's noise behavior is clearly discernible. In these experiments the feedback resistor of the input stage was altered by mechanically reducing the width of the thin-film element.

A comparison of the minimum noise figure plotted in Fig. 11(b) with that based on the theoretically obtained

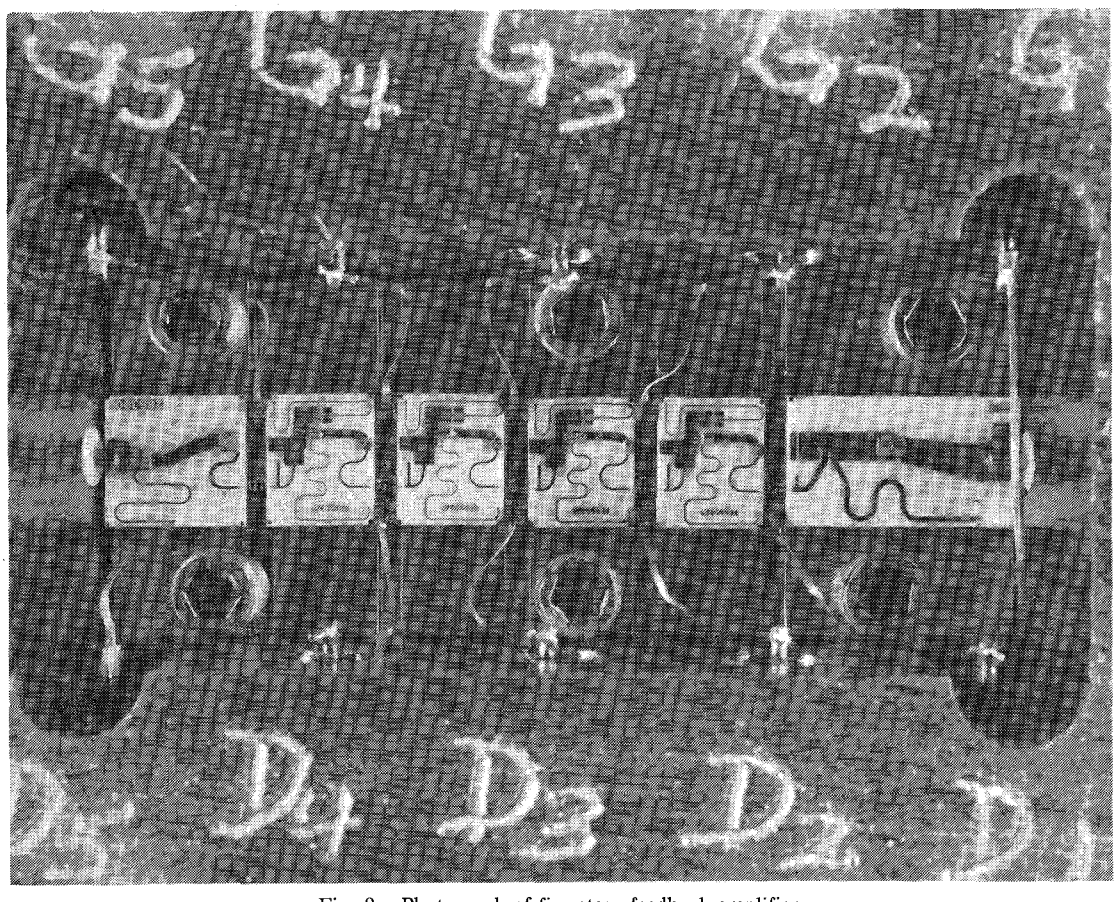

Fig. 9. Photograph of five-stage feedback amplifier.

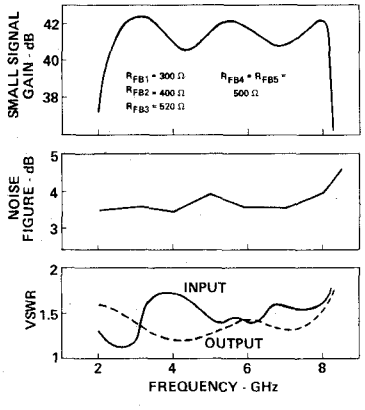

Fig. 10. Small-signal gain, noise figure, and VSWR performance of the five-stage amplifier.

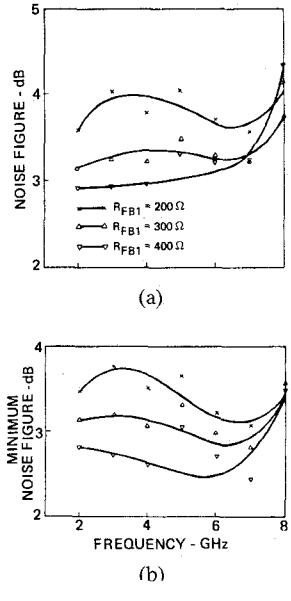

Fig. 11. Noise figure of the input stage for different feedback resistors. (a) Amplifier noise figure. (b) Optimized noise figure.

noise parameters (Fig. 7(b)) exhibits reasonably good agreement up to approximately 7 GHz. The deviation evident at higher frequencies is partially due to the fact that the degree of difficulty to achieve the conditions for optimum noise match increased with frequency. In addition the tuner used in our experiments had losses and was itself a source of noise making critical adjustments very difficult.

IV. Conclusion

A set of transformation formulas for the equivalent noise parameters of the basic feedback amplifier have been developed. Based on these formulas the influence of certain circuit elements such as the feedback resistor and the electrical length of the drain transmission line on minimum noise figure have been investigated. Important design tradeoffs between noise figure, small-signal gain and VSWR performance resulted from these studies. They point out the influence of the feedback resistor's magnitude and the

drain transmission line's characteristics on the amplifier's performance.

Finally, experimental data in support of the theoretical results has been presented. A comparison between calculated and measured minimum noise figures shows reasonably good agreement. The measurements were performed on a single-ended five-stage feedback amplifier. Its overall performance demonstrates the application feasibility of the feedback principle to single-ended wide-band low-noise amplification.

APPENDIX

The equivalent circuit of the principal feedback amplifier with its outside noise voltage and noise current sources is shown in Fig. 3(a). It consists of the main two-port and a parallel feedback loop between input and output. The main two-port is represented in the one-generator equivalent circuit form.

Using the symbols of Fig. 3(a), the total input and output currents are given by

$$I_1^{II} = (Y_{11}+Y_{FB})V_1 + (Y_{12}-Y_{FB})V_2 - (Y_{11}v_1 + Y_{FB}v_{FB}) + i_1 \tag{A.1a}$$

$$I_2^{II} = (Y_{21}-Y_{FB})V_1 + (Y_{22}+Y_{FB})V_2 - (Y_{21}v_1 - Y_{FB}v_{FB}). \tag{A.1b}$$

Equations (A.1a) and (A.1b) can be rewritten in matrix representation and may take the form

$$\begin{bmatrix} I_1^{II} - i_1 + Y_{11}\, v_1 + Y_{FB}v_{FB} \\ I_2^{II} + Y_{21}\, v_1 - Y_{FB}v_{FB} \end{bmatrix} = \begin{bmatrix} (Y_{11}+Y_{FB}) & (Y_{12}-Y_{FB}) \\ (Y_{21}-Y_{FB}) & (Y_{22}+Y_{FB}) \end{bmatrix} \begin{bmatrix} V_1 \\ V_2 \end{bmatrix}. \tag{A.2}$$

The admittance matrix (A.2) is then easily converted into the chain matrix relating the input and output quantities

$$\begin{bmatrix} V_1 \\ I_1^{II} - i_1 + Y_{11}v_1 + Y_{FB}v_{FB} \end{bmatrix} = -\frac{1}{(Y_{21}-Y_{FB})} \begin{bmatrix} (Y_{22}+Y_{FB}) & 1 \\ \Delta_y & (Y_{11}+Y_{FB}) \end{bmatrix} \cdot \begin{bmatrix} V_2 \\ -(I_2^{II} + Y_{21}v_1 - Y_{FB}v_{FB}) \end{bmatrix} \tag{A.3}$$

with

$$\Delta_y = (Y_{22}+Y_{FB})(Y_{11}+Y_{FB}) - (Y_{12}-Y_{FB})(Y_{21}-Y_{FB}). \tag{A.4}$$

Separating the signal from the noise quantities, we define

$$V_1 = V_1^I + v_1^I \tag{A.5a}$$

$$I_1^{II} = I_1^I + i_1^I \tag{A.5b}$$

and by substituting (A.5) into (A.3) we obtain the chain matrix of the input noise parameters

$$\begin{bmatrix} v_1^I \\ i_1^I - i_1 + Y_{11}v_1 + Y_{FB}v_{FB} \end{bmatrix} = -\frac{1}{(Y_{21}-Y_{FB})} \begin{bmatrix} (Y_{22}+Y_{FB}) & 1 \\ \Delta_y & (Y_{11}+Y_{FB}) \end{bmatrix} \cdot \begin{bmatrix} 0 \\ -(Y_{21}v_1 - Y_{FB}v_{FB}) \end{bmatrix}.$$

They can be written in the form

$$v_1^I = a_{11}\left(v_1 - \frac{Y_F}{Y_{21}}v_{FB}\right) \tag{A.7a}$$

$$i_1^I = a_{21}(v_1 - v_{FB}) + i_1 \tag{A.7b}$$

where

$$a_{11} = \frac{Y_{21}}{Y_{21}-Y_{FB}} \tag{A.7c}$$

$$a_{21} = Y_{FB}\frac{Y_{11}+Y_{21}}{Y_{21}-Y_{FB}}. \tag{A.7d}$$

Since i_1 and v_1 are correlated with each other, it is necessary to define

$$i_1 = i_n + Y_{cor}v_1 \tag{A.8}$$

where i_n is that part of the current i_1 that is not correlated with v_1. The factor Y_{cor} is the well-known correlation admittance.

Replacing i_1 in (A.7b) by (A.8) the total noise current takes the form

$$i_1^I = i_n + (a_{21}+Y_{cor})v_1 - a_{21}v_{FB} \tag{A.9}$$

its mean-square value is then given by

$$\overline{|i_1^I|^2} = \overline{|i_n|^2} + |a_{21}+Y_{cor}|^2\overline{|v_1|^2} + |a_{21}|^2\overline{|v_{FB}|^2}. \tag{A.10a}$$

The mean-square value of the noise input voltage obtained from (A.7a) is

$$\overline{|v_1^I|^2} = |a_{11}|^2\left(\overline{|v_1|^2} + \left|\frac{Y_{FB}}{Y_{21}}\right|^2\overline{|v_{FB}|^2}\right). \tag{A10.b}$$

The correlation admittance of the amplifier is defined as

$$Y_{cor}^I = \frac{\overline{i_1^I(v_1^I)^*}}{\overline{|v_1^I|^2}} \tag{A.11}$$

with

$$\overline{i_1^I(v_1^I)^*} = a_{11}^*\left[(a_{21}+Y_{cor})\overline{|v_1|^2} + a_{21}\frac{Y_{FB}^*}{Y_{21}^*}\overline{|v_{FB}|^2}\right] \tag{A.12}$$

and (A.10b) the correlation admittance is given by

$$Y_{cor}^I = \frac{a_{21}\left[\overline{|v_1|^2} + \frac{Y_{FB}^*}{Y_{21}^*}\overline{|v_{FB}|^2}\right] + Y_{cor}\overline{|v_1|^2}}{a_{11}\left[\overline{|v_1|^2} + \left|\frac{Y_{FB}}{Y_{21}}\right|^2\overline{|v_{FB}|^2}\right]}. \tag{A.13}$$

In order to determine $\overline{|i_n^I|^2}$ we make use of the identity

$$\overline{|i_n|^2}\ \overline{|v|^2} = \overline{|i|^2}\ \overline{|v|^2} - |\overline{iv^*}|^2. \tag{A.14}$$

Substituting (A.10) into (A.14) we obtain

$$\overline{|i_n^I|^2}\ \overline{|v_1^I|^2} = \overline{|i_n|^2}|a_{11}|^2\left(\overline{|v_1|^2} + \left|\frac{Y_{FB}}{Y_{21}}\right|^2 \overline{|v_{FB}|^2}\right) + \left|a_{11}\left(a_{21}\frac{Y_{21}-Y_{FB}}{Y_{21}} - Y_{cor}\right)\right|^2 \overline{|v_1|^2}\ \overline{|v_{FB}|^2} \tag{A.15}$$

and thus the mean square of the uncorrelated portion of the total noise current

$$\overline{|i_n^I|^2} = \overline{|i_n|^2} + \frac{\left|a_{21}\frac{Y_{21}-Y_{FB}}{Y_{21}} - \frac{Y_{FB}}{Y_{21}}Y_{cor}\right|^2 \overline{|v_1|^2}\ \overline{|v_{FB}|^2}}{\overline{|v_1|^2} + \left|\frac{Y_{FB}}{Y_{21}}\right|^2 \overline{|v_{FB}|^2}}. \tag{A.16}$$

Using the well-known Nyquist formulas

$$\overline{|v_1|^2} = 4kT_0\Delta f R_n \tag{A.17a}$$

$$\overline{|i_n|^2} = 4kT_0\Delta f G_n \tag{A.17b}$$

$$\overline{|v_{FB}|^2} = 4kT_0\Delta f R_{FB} \tag{A.17c}$$

we are now able to rewrite the equivalent noise quantities in terms of the noise resistance R_n, the noise conductance G_n, the correlation admittance Y_{cor} and the feedback resistance R_{FB}

$$R_n^I = \frac{\overline{|v_1^I|^2}}{4kT_0\Delta f} = \left|\frac{Y_{21}}{Y_{21}-Y_{FB}}\right|^2\left(R_n + \left|\frac{Y_{FB}}{Y_{21}}\right|^2 R_{FB}\right) \tag{A.18a}$$

$$G_n^I = \frac{\overline{|i_n^I|^2}}{4kT_0\Delta f} = G_n + |Y_{11}+Y_{21}-Y_{cor}|^2\frac{\left|\frac{Y_{FB}}{Y_{21}}\right|^2 R_n R_{FB}}{R_n + \left|\frac{Y_{FB}}{Y_{21}}\right|^2 R_{FB}} \tag{A.18b}$$

$$Y_{cor}^I = \frac{\overline{i_1^I (v_1^I)^*}}{\overline{|v_1^I|^2}} = Y_{cor} + (Y_{11}+Y_{21}-Y_{cor})\frac{\frac{Y_{FB}}{Y_{21}}R_n + \left|\frac{Y_{FB}}{Y_{21}}\right|^2 R_{FB}}{R_n + \left|\frac{Y_{FB}}{Y_{21}}\right|^2 R_{FB}}. \tag{A.18c}$$

Acknowledgment

The author wishes to thank R. Pereira, who performed the measurements and whose outstanding skills in tuning the amplifiers greatly contributed to the success of this program. Thanks go also to W. T. Wilser who edited the manuscript and supervised the fabrication of the GaAs MESFET's. The author is indebted to P. Hutchison who typed the complicated formulas.

References

[1] K. B. Niclas, "Compact multi-stage single-ended amplifiers for S-C band operation," in *1981 MTT-S Int. Microwave Symp. Dig. Tech Papers*, pp. 132–134.

[2] K. B. Niclas, W. T. Wilser, R. B. Gold, and W. R. Hitchens, "The matched feedback amplifier: Ultrawide-band microwave amplification with GaAs MESFET's," *IEEE Trans. Microwave Theory Tech.*, vol. MTT-28, pp. 285–294, Apr. 1980.

[3] L. Besser, "Stability considerations of low-noise transistor amplifiers with simultaneous noise and power match," in *1975 Int. Microwave Sym. Dig. Tech. Papers*, pp. 327–329.

[4] G. Vendelin, "Feedback effects on the noise performance of GaAs MESFET's," in *1975 Int. Microwave Symp., Dig. Tech. Papers*, pp. 324–326.

[5] J. Engberg, "Simultaneous input power match and noise optimization using feedback," in *European Microwave Conf., Dig. Tech. Papers*, pp. 385–389, Sept. 1974.

[6] R. Sittner, "Einfluss von Rückkopplungen auf das Rauschen von Verstärkern," *Nachrichtentech. Fachberichte*, vol. 2, pp. 41–48, 1955.

[7] K. Hartmann and M. J. O. Strutt, "Changes of the four noise parameters due to general changes of linear two-port circuits," *IEEE Trans. Electron Devices*, vol. ED-20, pp. 874–877, Oct. 1973.

[8] S. Iversen, "The effect of feedback on noise figure," *Proc. IEEE*, vol. 63, pp. 540–542, Mar. 1975.

[9] H. Rothe and W. Dahlke, "Theory of noisy fourpoles," *Proc. IRE*, vol. 44, pp. 811–818, June 1956.

[10] W. Dahlke, "Transformationsregeln für rauschende Vierpole," *Arch. Elek. Übertragung*, vol. 9, pp. 391–401, Sept. 1955.

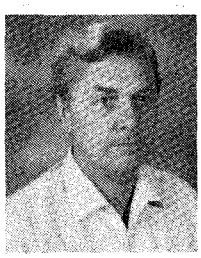

Karl B. Niclas (M'63–SM'81) received the Dipl.-Ing. and Doctor of Engineering degrees from the Technical University of Aachen, Aachen, Germany, in 1956 and 1962, respectively.

From 1956 to 1962 he was with the Microwave Tube Laboratory at the Telefunken G.m.b.H. Tube Division, Ulm-Donau, Germany. He was engaged in research and development on ultra-low-noise and medium-power traveling-wave tubes. In 1958 he became Head of the company's Traveling-Wave Tube Section and Assistant Manager of the Microwave Tube Laboratory. From 1962 to 1963 he was associated as a Senior Project Engineer with General Electric Microwave Laboratory, Stanford, CA. His work was mainly concerned with theoretical and experimental investigations of single-reversal focused low-noise traveling-wave tube amplifiers, and resulted in the first lightweight amplifier of this type. In 1963 he joined the Technical Staff of Watkins-Johnson Company, Palo Alto, CA, and is presently Consultant to the Vice President, Devices Group. His present research efforts are primarily focused on advanced GaAs FET amplifiers, broad-band power combining techniques, and wide-band GaAs FET oscillator concepts. From 1967 to 1976 he was Manager of the company's Tube Division. Before that, he was Head of the Low-Noise Tube R & D Section, and prior to that he was engaged in a research program on new concepts for achieving high efficiency in traveling-wave tubes. He is the author of numerous papers and holds a number of patents.

Dr. Niclas received the outstanding publications award in 1962 of the German Society of Radio Engineers.